

A Numerical Modeling on Light I-V Curves of Hetero-Junction Amorphous Silicon Solar Cells

Hu Zhi-Hua^{1,*}, Hu Shu-Yu²

¹ Key Lab.of Advanced Technology & Preparation for Renewable Energy Materials, State Ministry of Education, Yunnan Key Lab.of Rural Energy Engineering, School of Energy and Environmental Sciences, Yunnan Normal University, Kunming, 650092, China

² College of Mechanical and Electronic Engineering, China University of Petroleum, Qingdao, 266580, China

*E-mail: 1049173841@qq.com

Received: 29 March 2021 / Accepted: 11 May 2021 / Published: 30 June 2021

In this work, AMPS-D (Analysis of Microelectronic and Photonic Structures) mode was used to simulate hetero-junction amorphous silicon solar cell. The influence of energy band mismatch at p/i interface and Schottky barrier at TCO/p or n/metal interfaces on light I-V characteristics was investigated on a solar cell with a pin structure of TCO/p-a-SiC:H/i-a-Si:H/n-a-Si:H/metal. Simulation shows that the energy band mismatch at p/i interface is the main cause of the abnormal bending of the light I-V curves in a voltage range of less than the open circuit voltage (V_{oc}). Schottky barrier E_p at TCO/p or E_n at n/metal interfaces causes the light I-V curve bending in a voltage range higher than V_{oc} .

Keywords: AMPS-1D, hetero-junction, amorphous silicon, solar cell

1. INTRODUCTION

The light current-voltage (I-V) curves of the high quality amorphous silicon solar cells are close to the dark curves of ideal diode, and light-dark I-V curves basically follow the superposition principle. However, the interface problems may lead to poor performance of amorphous silicon solar cells, resulting in a decrease in open-circuit voltage and fill factor [1]. In fact, abnormal behavior is common in light I-V characteristic curve of hetero-junction solar cells [2], scholars nominates it as curve rollover, curve crossover, V_{oc} shift, and roll-under phenomenon [3]. In this paper, these abnormal phenomena can be clarified in two types, one occurring far over the open circuit voltage (V_{oc}), and the other occurring near or below the V_{oc} . Based on the analysis of device physics and manufacture processes, the authors of this work hold that all these abnormal behaviors are mainly caused by various interface problems. In this paper, the AMPS-1D (Analysis of Microelectronic and Photonic Structures) [4]

developed by Penn State University was employed to module the TCO/p, p/i and n/metal interfaces in amorphous silicon solar cells. The influence of energy band offset at p/i interface, interface defects concentration and barrier height of n/metal interface on light I-V characteristics curves were simulated for hetero-junction amorphous silicon solar cells.

2. DEVICE MODEL AND PARAMETER SETTING

2.1. Device and Materials Model

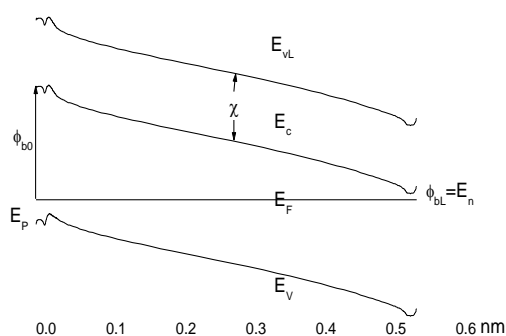


Figure 1. Energy band diagram of a TCO/p-a-SiC:H/i-a-Si:H/n-a-Si:H/metal a-Si solar cell

Fig.1 shows the energy band diagram of a hetero-junction pin a-Si solar cell. In Fig.1, ϕ_{b0} is the difference between Fermi energy level of TCO and conduction band of P layer ; E_P is the contact barrier (for hole) at the TCO/P interface; E_{vL} is the vacuum energy level; χ is the electron affinity (χ plus electron activation energy E_a is so-called work function W); ϕ_{bL} (E_n) is the n/metal interface contact barrier; the scale at the bottom of the figure is the cell thickness dimension. AMPS-1D is optional in DOS (Defect of State) and Life Time mode for semiconductor electronic description[5]. In this work, DOS mode was used in all calculation. In DOS mode, the electronic states of semiconductor can be divided into conduction band states, conduction band extended states, valence band states, valence band tail localized states and gap localized states[6]. The valence band tail localized states are mainly originated from bonds angle distortion, and band gap localized states are mainly caused by hanging bonds. Dual Gaussian functions with a background of average distribution were used to describe density of band gap localized states corresponds to donor-like states and acceptor-like states[7] respectively, and donor-like states are beneath and the acceptor-like states are above. For amorphous silicon, an exponential was used to describe the tail localized states. Phosphor and boron Doped in N layer and P layer are totally ionized[8], i.e $N_D^+ = N_D$, $N_A^- = N_a$.

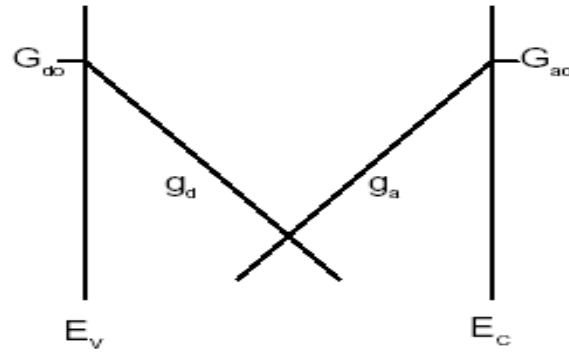


Figure 2. Band tail defect states density distribution

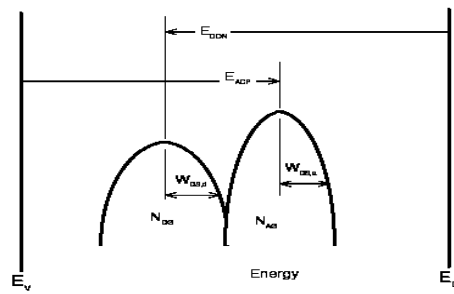


Figure 3. Dual Gaussian distribution of band gap defect states density

Fig.2 shows the distribution of band tail defect states density, where:

$$g_a(E) = G_{a0} \exp[(E_c - E) / E_A]$$

$$g_d(E) = G_{d0} \exp[(E - E_v) / E_D]$$

E_A and E_D represent characteristic energy for conduction band and valence band tail respectively.

Fig.3 shows the dual Gaussian distribution of band gap defect states density[9] provided by AMPS for describing the density of states of defects in amorphous silicon. $N_{DG}(N_{AG})$ represents the Gaussian distribution of donor-like (acceptor-like) defect states density (cm^{-3}) [10], $W_{DS, d}(W_{DS, a})$ and E_{DON} (E_{ACP}) represent the half-width of Gaussian peak of donor-like (acceptor-like) state and the energy difference between Gaussian peak of donor-like (acceptor-like) and edge of conduction band (valence band)[11], respectively.

2.2. Parameters Settings

The device used for simulation is a p-i-n hetero-junction solar cell, and the light illuminates on the p-type side. The p-type window layer is hydrogenated amorphous silicon carbon (a-SiC:H) with a mobility band gap of 1.96 eV[12]. The photoelectric characteristic parameters of all the device component layers are shown in table 1. The Electron affinity χ of a-SiC:H is setting as 3.90 eV, 0.10 eV smaller than that of hydrogenated amorphous silicon (a-Si:H), which means that, the energy band discontinuity (1.96-1.80 eV) at the p/i interface offsets by 0.10 eV on the valence band and 0.06 eV on

the conduction band, respectively.

Simulation condition is AM1.5,100mW/cm² at a temperature of 25°C. The absorption coefficients of intrinsic a-Si:H layer are expressed by the following equation[13]:

$$\alpha(h\nu) = B \left[\frac{(h\nu - E_g)^2}{h\nu} \right]$$

the values of B and E_g in this equation are shown in table 1.

Table 1. Parameters Setting in AMPS-1D

Parameters	P-layer (a-SiC:H)	I-layer (a-Si:H)	N-layer (nc-Si:H)
Thickness (nm)	8	500	25
Mobility band edge gap E _μ (eV)	1.96	1.80	1.80
Optical band gap E _g (eV)	1.80	1.72	1.72
B in Coeff. equation (cm ^{-1/2} eV ^{-1/2})	1050	800	700
Electron affinityχ(eV)	3.90	4.00	4.00
N _D in N-layer (cm ⁻³)	0	0	5E19
N _A in P-layer (cm ⁻³)	5E19	0	0
Accept. Activation Energy E _{AA} (eV)	0.25		
Donor Activation Energy E _{AD} (eV)			0.10
Effective states density (cm ⁻³)	2.5E20	2.5E20	2.5E20
Band gap defect states density N _{DG} and N _{AG} (cm ⁻³)	5E17	5E15	5E17
E _{DON} (eV)	1.12	1.12	1.12
E _{ACP} (eV)	1.12	1.12	1.12
E _D in Coeff. equation (eV)	0.05	0.05	0.05
E _A in Coeff. Equation (eV)	0.03	0.03	0.03
G ₀₀ in Coeff. equation (eV)	1.0E21	1.0E21	1.0E21
G _{a0} in Coeff. equation (eV)	1.0E21	1.0E21	1.0E21

3. RESULT AND DISCUSSION

3.1. Effects of p/i Energy Band Gaps of Buffer Layer

In an earlier work[14], the author had analyzed the influence of defects concentration at p/i interface on performance of amorphous silicon solar cells by inserting a 1nm thick buffer layer in between p/i layers with varied defects concentration. As a conclusion, the leakage current increases with increasing defects concentration, therefore deteriorate open-circuit voltage (V_{oc}) and fill factor of solar cells. In addition to these interface defects concentration, are there any other physical factors affect the photoelectric characteristics of a-Si:H solar cells? Then the energy band gaps come into this work.

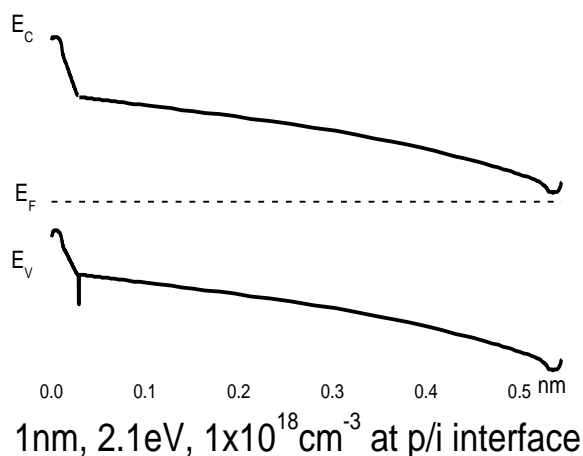


Figure 4. Energy diagram of a TCO/p-a-SiC:H/i-a-Si:H/n-a-Si:H/metal; A-Si solar cell with a wide band gap interface buffer layer

An ideal amorphous silicon solar cell with a 1nm thick , 1.8eV band gap and $1 \times 10^{14} \text{ cm}^{-3}$ defects concentration buffer layer was constructed as a base model. The major materials and device parameters are shown in table-1. On the basis of this model, the defects concentration of this 1nm thick buffer layer was adjusted to $1 \times 10^{18} \text{ cm}^{-3}$ together with a varied band gap from 1.8eV to 2.1eV. The energy band mismatches between the buffer layer and the P , I layers were adjusted by the Electron affinity χ of each layers. The energy band broadening of buffer layer is mainly allocated to the valence band. Figure 4 shows the equilibrium energy diagram of the device with a buffer layer inserted. The light I-V curves of devices with different band gaps are shown in Figure 5.

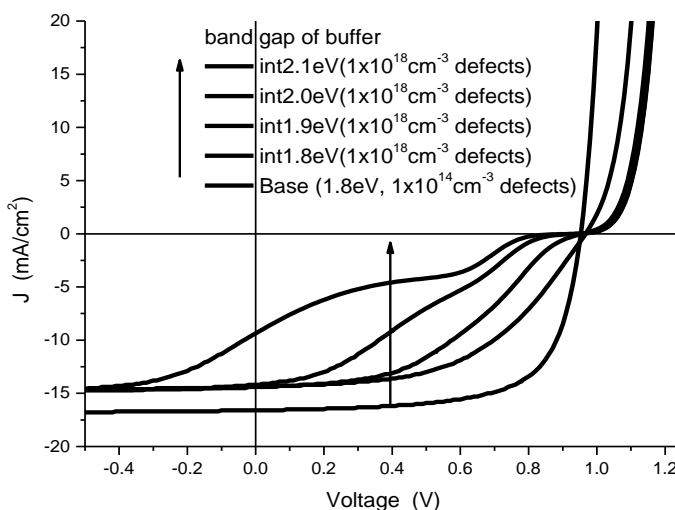


Figure 5. Light I-V curves of solar cells with varied band gaps of the buffer layer

As seen in Fig.5, the insertion of the buffer layers with wide band gap and high defects concentration in between the p/i interface causes the abnormal turning of the light I-V curve near and beneath the V_{OC} . Thus, p/i interface is dominant interface of amorphous silicon solar cell. In fact, the author had reported [14] that, the defects at the p/i interface cause energy band to bend, and the Fermi Energy Level thus be pinned to the center of the band gap at the p/i Interface (as shown in Fig. 4), which reduces the built-in electric field and the collection efficiency of photo-generated carriers. Meanwhile, the valence band mismatch caused by the wider band gap interface layer forms a potential barrier to the photo-generated hole at the p/i interface, which hinders the collection of the photo-generated hole. This hole impedance causes most of abnormal behaviors near and beneath V_{OC} , which significantly deteriorate the performance, especially fill factor or energy conversion efficiency of photovoltaic devices.

3.2. Effects of TCO/p and n/metal Interface Carrier Barrier

In addition to the p/i interface, the front and back contact are also important for amorphous silicon solar cells. For an ideal Ohmic contact, there should be no Schottky barrier between the interfaces that impedes the collection of carriers[15]. However, there is a work function difference at TCO/p-layer and n/metal interface, which forms a Schottky barrier. All these interfaces have a large number of interface states which lead to a Fermi energy level pinning. We had simulated the effects of TCO/p and n/metal Schottky barrier's height, E_p and E_n respectively (shown in Fig.6) on the photoelectric characteristics of pin solar cells. Fig.8 shows the results.

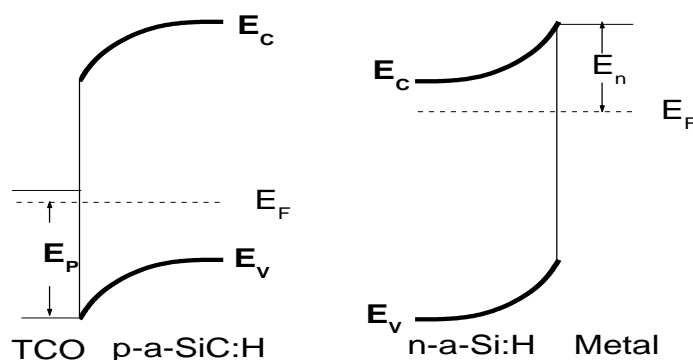


Figure 6. Schottky barrier's height, E_p and E_n at TCO/p and n/metal interface

Fig. 7 shows the light I-V curves of solar cells with different TCO/p (a) and n/metal (b) Schottky barrier heights (E_p and E_n). It is seen that both E_p and E_n affect the open-circuit voltage and the filling factor. On the I-V curves, when either E_p or E_n reaches or exceeds 0.6 eV, the I-V curves appear to bend beyond the V_{OC} [16]. The effect of E_p and E_n are theoretically equal in theory, but the TCO/p interface is more dominant considering the asymmetry of carriers generation and collection in amorphous silicon solar cells. Practically, various interface problems may exist in entire process and I-V curves may occur

bending and turning in any voltage range. Combined the effects of energy band mismatch at p/i interface and Schottky barrier at TCO/p or n/metal interfaces together, an more common abnormal light I-V curves were simulated as shown in Fig.8. In Fig.8, it is seen that I-V curve's bending occurs both in voltage range less and higher than open circuit voltage (V_{oc}), which is originated from p/i interface and $E_p \sim \text{TCO/p}$ or $E_n \sim \text{n/metal}$ interface respectively.

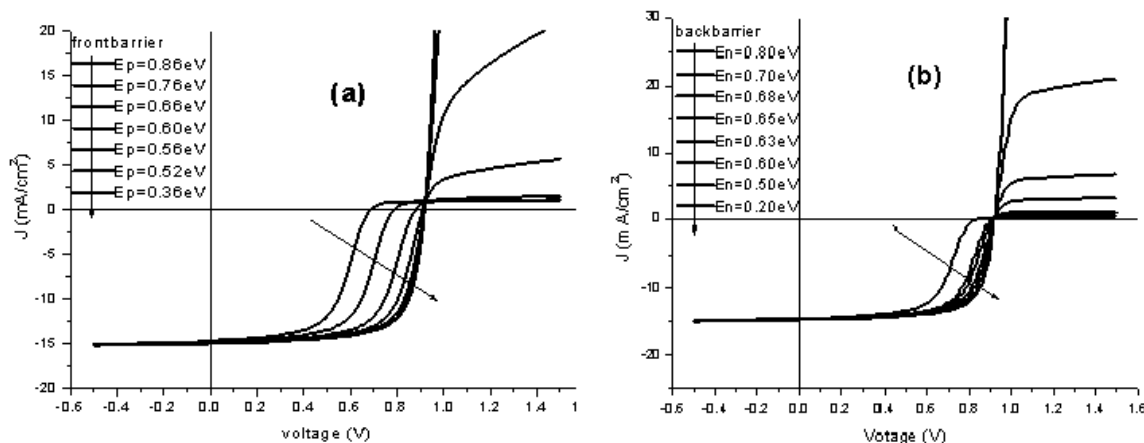


Figure 7. Effects of E_p and E_n on the light I-V curves of solar cells

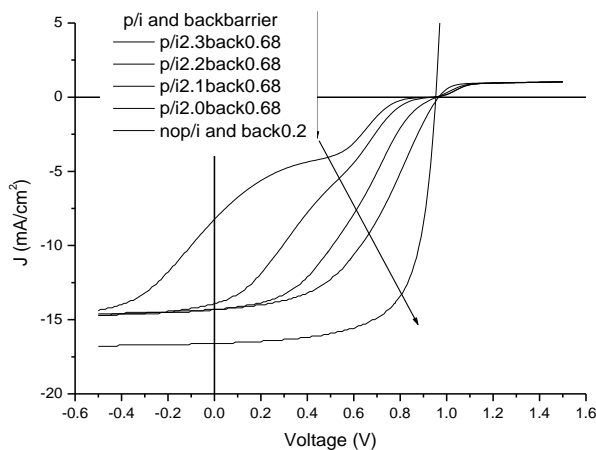


Figure 8. Effects of energy band mismatch at p/i interface and E_n at n/metal interface on light I-V curves

4. CONCLUSION

AMPS-D was used to simulate the influence of energy band mismatch at p/i interface and Schottky barrier at TCO/p or n/metal interfaces on light I-V characteristics of a hetero-junction amorphous silicon solar cell with a pin structure of TCO/p-a-SiC:H/i-a-Si:H/n-a-Si:H/metal. Simulation shows that the energy band mismatch at p/i interface is the main cause of the abnormal bending of the

light I-V curves in a voltage range of less than the open circuit voltage (V_{oc}). Schottky barrier E_p at TCO/p or E_n at n/metal interfaces causes the light I-V curve bending in a voltage range higher than V_{oc} .

References

1. H. Steibig, T. Eickhoff, J. Zimmer, C. Beneking and H. Wagner, Proceeding MRS Symposium, (1996), 855.
2. T. McMahon and A. Fahrenbruch, Proceeding 28th IEEE Photovoltaic Spec. Conf. (2000), 539.
3. X. Deng, W. Wang and X. Liao, *International Journal of Modern Physics B*, 16 (2002) 57.
4. For AMPS-1D please see: <http://www.empri.psu.edu/amps>.
5. J. K. Arch, F. A. Rubinelli, J. Y. Hou, and S. J. Fonash, *J. Appl. Phys.* 69 (1991) 7057.
6. Petr Sládek, Pavel Stáhel, Pere Roca I. Cabarrocas, Philippe Morin, *Philosophical Magazine B*, 77(4) (1998) 1049.
7. John G Shaw and Michael Hack, *Journal of Applied Physics*, 64 (9) (1988) 4562.
8. X. Xu, J. Yang, A. Banerjee, S. Guha, K. Vasanth and S. Wagner, *Appl. Phys. Lett.* 67 (16) (1995) 2323.
9. T. Itoh, Y. Hasegawa, T. Fujiwara, A. Masuda and S. Nonomura, *Journal of Non-Crystalline Solids*, 338-340 (2004) 123.
10. F. Sanchez-Sinencio and R. Williams, *Journal of Applied Physics*, 54 (1983) 2757.
11. Zhe Li, Xiwen Zhang and Gaorong Han, *Applied Materials Science*, 01 (2010) 144.
12. X.X. Zheng, X.D. Zhang, S.S. Yang, S.Z. Xu, C.C. Wei and Y. Zhao, *Solar Energy Materials and Solar Cells*, 06 (2012) 15.
13. Lei Zhao, Bending Zhao, Baojun Yan, Hongwei Diao, Yanli Mao and Wenjing Wang, *Materials Science in Semiconductor Processing*, (2013) 363.
14. Z. Hu and X. Liao, *Acta Physica* (in Chinese), 54 (2005), 2302
15. Liu, XJ, Yin, JC, Zhang, JW, Li, M, Yang, PZ and Hu, ZH, *International Journal of Electrochemical Science*, 11, (2016), 12.
16. Guifang Han, Sam Zhang, Pablo P. Boix, Lydia Helena Wong, Lidong Sun, Shui-Yang Lien, *Progress in Materials Science*, 87(2017), 246.